Hindawi
Advances in Civil Engineering
Volume 2020, Article ID 3696489, 10 pages
https://doi.org/10.1155/2020/3696489

Research Article

Anchor Stress and Deformation of the Bolted Joint under Shearing

Hang Lin,[1,2] **Youyan Zhu**,[1] **Jianyu Yang**,[3] **and Zhijie Wen**[2]

[1]*School of Resources and Safety Engineering, Central South University, Changsha, Hunan 410083, China*
[2]*State Key Laboratory of Mining Disaster Prevention and Control Co-founded by Shandong Province and the Ministry of Science and Technology, Shandong University of Science and Technology, Qingdao 266590, China*
[3]*School of Civil Engineering, Changsha University of Science and Technology, Changsha 410114, China*

Correspondence should be addressed to Jianyu Yang; yangjianyuhu@126.com and Zhijie Wen; sdust0532@gmail.com

Received 6 July 2019; Revised 11 September 2019; Accepted 20 September 2019; Published 20 January 2020

Academic Editor: Hayri Baytan Ozmen

Bolts are widely used in rock mass engineering, wherein the bolt support improves the safety and stability of the rock mass. To reveal the mechanical behavior of the bolt and failure mechanism of the bolted joint in the shearing process, a direct shear test was conducted by changing the state of grouting, number of bolt, and inclination angle of the bolt. The change in the axial force of the anchor in the shearing process was evaluated by conducting a strain gauge test, and the mechanical behavior of the bolt under the external force was studied. The results showed that under the same normal stress, the yield displacement of the bolt decreased and the stiffness of the joint gradually increased with increased number of bolts. At the same number of bolts, their yield displacement increased with increased normal stress. Analysis further revealed that grouting on the joint improved the force condition of the bolt, increased the yield displacement of the bolt, and coordinated the deformation of the grouting body and bolt, thereby improving the shear strength of the joint. Lastly, when the anchor angles differed, the axial pulling resistance of the anchor changed, and the yield displacement of the anchor with 45° inclination was <90°. The yield displacement of the bolt showed that the supporting effect of the bolt with a 45° inclination was better than that of the bolt with a 90° inclination.

1. Introduction

Fractured rock masses exist extensively in geotechnical engineering [1–7]. Many researches have been done on the mechanics of rock joint. Lin et al. [8] investigated the effect of different confining stresses on the rock breaking of different joint angles. Jiang et al. [9] simulated series of direct shear tests on coplanar and noncoplanar jointed rocks using the PFC2D. The failure of joint will greatly affect the safety of rock mass [10–14]. Bolts are widely used in major projects such as steep slopes and tunnels as an important means of reinforcing the fractured rock masses [15–18]. Many scholars have conducted extensive research on the anchoring mechanism of bolts in rock masses and achieved many meaningful results [19–27]. Ge and Liu [28] studied the effects of different bolt angles, material properties, and friction angles on the shear strength of the joint and proposed a formula for estimating the shear strength of the bolted joint and the optimal anchor installation angle. Chen et al. [29] analyzed the axial and transverse deformations of the bolt in the shearing process and found that with increased strength of the surrounding rock or the normal stress, the shear strength of the joint contributed by the axial force of the bolt is reduced. Spang and Egger [30] studied the shear resistance of bolts in different materials and considered that one of the most important parameters affecting the shear resistance of anchored jointed rock masses is the deformability of the rock mass. Pellet and Egger [31] studied the shear resistance of bolts through theoretical methods and obtained the allowable deformation of the bolts with different installation angles. Haas [32] used various types of bolts to anchor into limestone and shale, and shear tests showed that the shear resistance of the joint surface after anchoring increased by approximately 3.7 times. According to the study of Grasselli et al. [33], the plastic hinge was formed when the shear displacement of the anchored rock mass reached a certain value, and the failure of the anchor rod was mainly from the pulling force

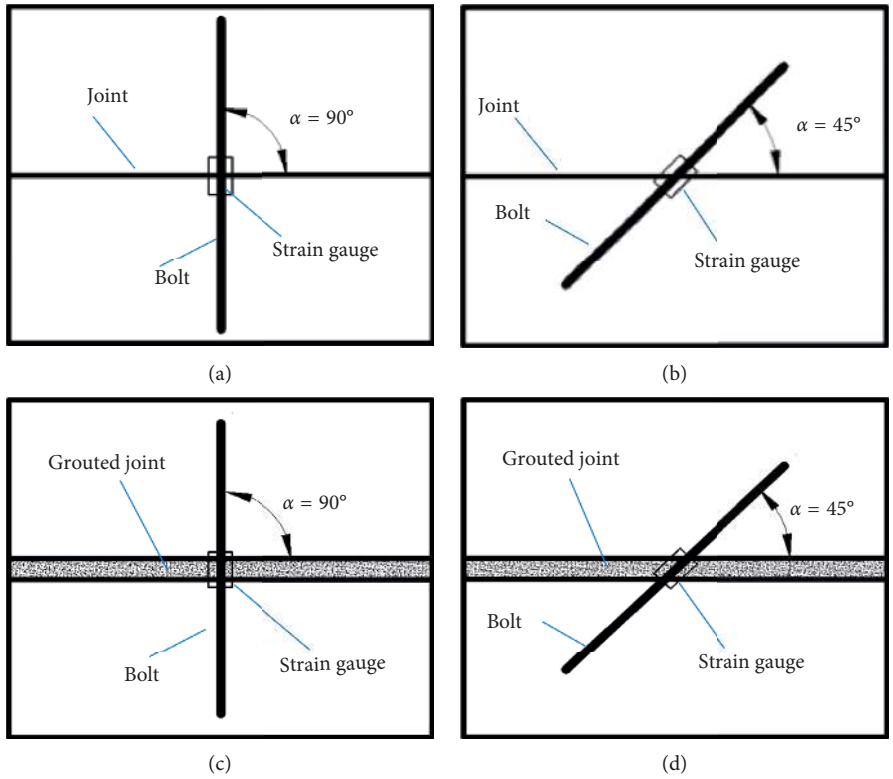

Figure 1: Schematic of the sample. (a) 90° and (b) 45° bolted nonfilled joints. (c) 90° and (d) 45° bolted grouted joints.

Figure 2: Joint sample. (a) Bolted nonfilled joint. (b) Bolted grouted joint.

concentrated between the two plastic hinges. The above studies focused on the improvement of the shear strength of the joint after anchoring. The stress deformation of the bolt itself during shearing is also important because such deformation affects the failure mode of the rock joint [34–36]. Discussing the deformation characteristics of the bolt in the shearing process is particularly necessary during the time when the bolt begins to deform during the shearing process and when the yield begins to occur, and how the axial drawing effect is exerted is also necessary. Based on the above considerations, the authors conducted the direct shear test, changed the number of bolts, the grouting state of the joint, and the inclination angle of the bolts. The deformation characteristics of the joint bolts were discussed.

2. Sample Preparation and Test Methods

Using a similar material to simulate the joint, a direct shear test was performed and the entire shear stress-shear displacement curve was recorded under a certain normal load [9, 37–43]. The white Portland cement numbered 425 and

muddy river sand with a particle size of 0.5 to 1.0 mm are used for sampling and then casted according to the ratio (mass ratio) cement : sand : water = 1 : 0.53 : 0.45 with the size of 150 × 150 × 120 mm. The test piece is divided into two pieces, the joint surface is laid straight, and the types of joints are divided into two categories: nonfilled and grouted joints. The specific model is shown in Figure 1 wherein the thickness of the grout is 8 mm. The inclined bolt exerts lateral shear resistance, and the axial pull effect of the bolt and anchor increases the strength of the joint because the support effect of the inclined bolt is better than that of the vertical bolt. To compare the effect of bolt inclination and bolt amount, the installation angle of the bolt is set to be 45° and 90°, and the number is approximately 1 to 3. The joints with bolts can then be categorized into bolted nonfilled and bolted grouted joints [44]. The bolt is simulated using the #11 wire with a length of 11 mm and a diameter of 3 mm. A BE120-5AA (11) strain gauge with a length of 5 mm and a width of 2 mm was attached onto the middle of the anchor rod. Joint samples are shown in Figure 2. The strain at the anchor point of the specimen was measured by the strain gauge, and then the deformation characteristics of the bolt at the joint can be obtained. During the production process, the bolt is inserted into the test piece before the cement mortar is solidified, and then the full-length bonded bolt is formed. Two central axes are defined and shown in Figure 3. The bolt is placed along the center axis 2. One bolt is positioned at the intersection of the center axes 1 and 2. Bolts 2 and 3 are located uniformly along the center axis 2 with the spacing of 50 and 37.5 mm, respectively. The grout is prepared with cement mortar with different proportions of the rock joint model, and the ratio (mass ratio) of the cement mortar is cement : sand : water = 1 : 1 : 0.35. When casting the simulated rock mass, a gap of thickness $\delta = 8$ mm is reserved in advance, and then the specimen is grouted after 4 to 5 days of curing. The specimen is placed in a constant temperature box for conservation. The sample after casting is shown in Figure 2.

To obtain the deformation characteristics of the bolt, the strain monitoring points were set in the middle of the bolt. Figure 3 shows that the epoxy resin was used to protect the strain gauges. Direct shear tests were performed under a certain normal stress. When grouting is done on the structure, the strain gauges are all buried in the grouting body. The test system is a RYL-600 microcomputer-controlled rock shear tester as shown in Figure 4. The tangential loading rate is set to 1 mm/min.

3. Analysis of Shear Test Results

3.1. Influence of the Number of Bolts. The number of bolts affects the mechanical behavior of the joint [45]. The relationship of the strain-shear displacement of the bolt is shown in Figure 5. During the shearing process, the bolt deforms along with the shearing misalignment, and the strain value of the corresponding measuring point of the bolt is measured. However, breaking during the shearing process is easy and the strain gauge is destroyed because of the thinness of the strain gauge wire. Figure 5(a) shows that no change occurs after the strain value increases to a certain value until the strain gauge breaks. Figure 5 shows that during the initial stage of shearing, the strain of the bolt does not change remarkably with increased shear displacement. At this time, the axial pull effect of the anchor rod plays a minor role, and the axial force is not considerably increased because in the early stage of shearing, the shear action of the joint is provided by the pin action of the bolt, and the shear resistance of joint is consistent with the results of the phenomenon presented by Chen et al. [46]. However, when the shear displacement exceeds a certain critical value, the strain of the bolt increases rapidly with increased shear displacement wherein this critical point corresponds to the yield point of the bolt. Comparing the shear stress-shear displacement curves of the bolted grouted joint (Figure 6), the grouted joint shear displacement corresponding to the critical point (Figure 5) is located at the half to the full of the peak shear displacement. For the convenience of description, the shear displacement of the corresponding joint when the bolt is yielded is referred to as the yield displacement (D_y). For the normal stress of 2.22 MPa, the corresponding yield displacements are δ_{s1}, δ_{s2}, and δ_{s3} for grouted joint with one, two, and three bolts, respectively. Through the above

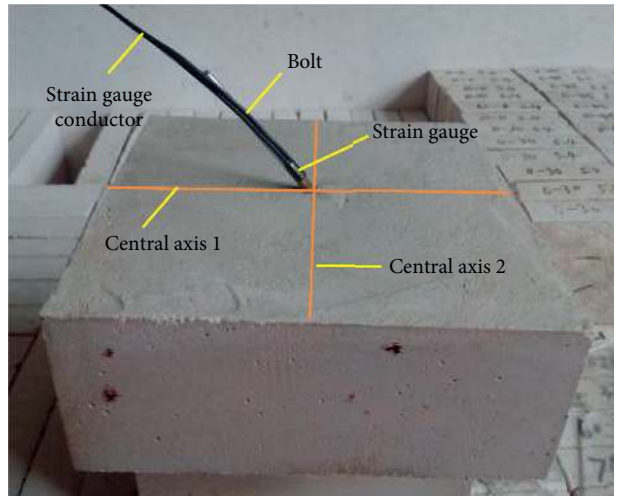

Figure 3: Center axis on the joint.

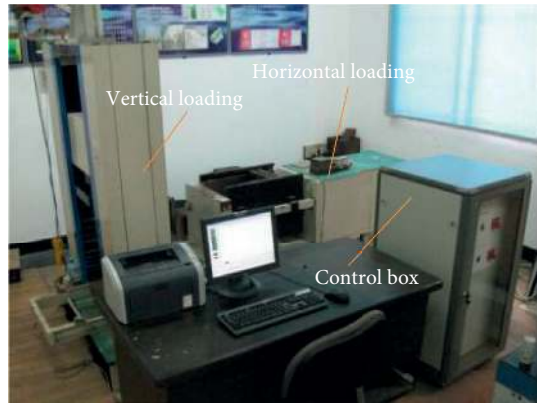

Figure 4: Direct shear instrument for rock.

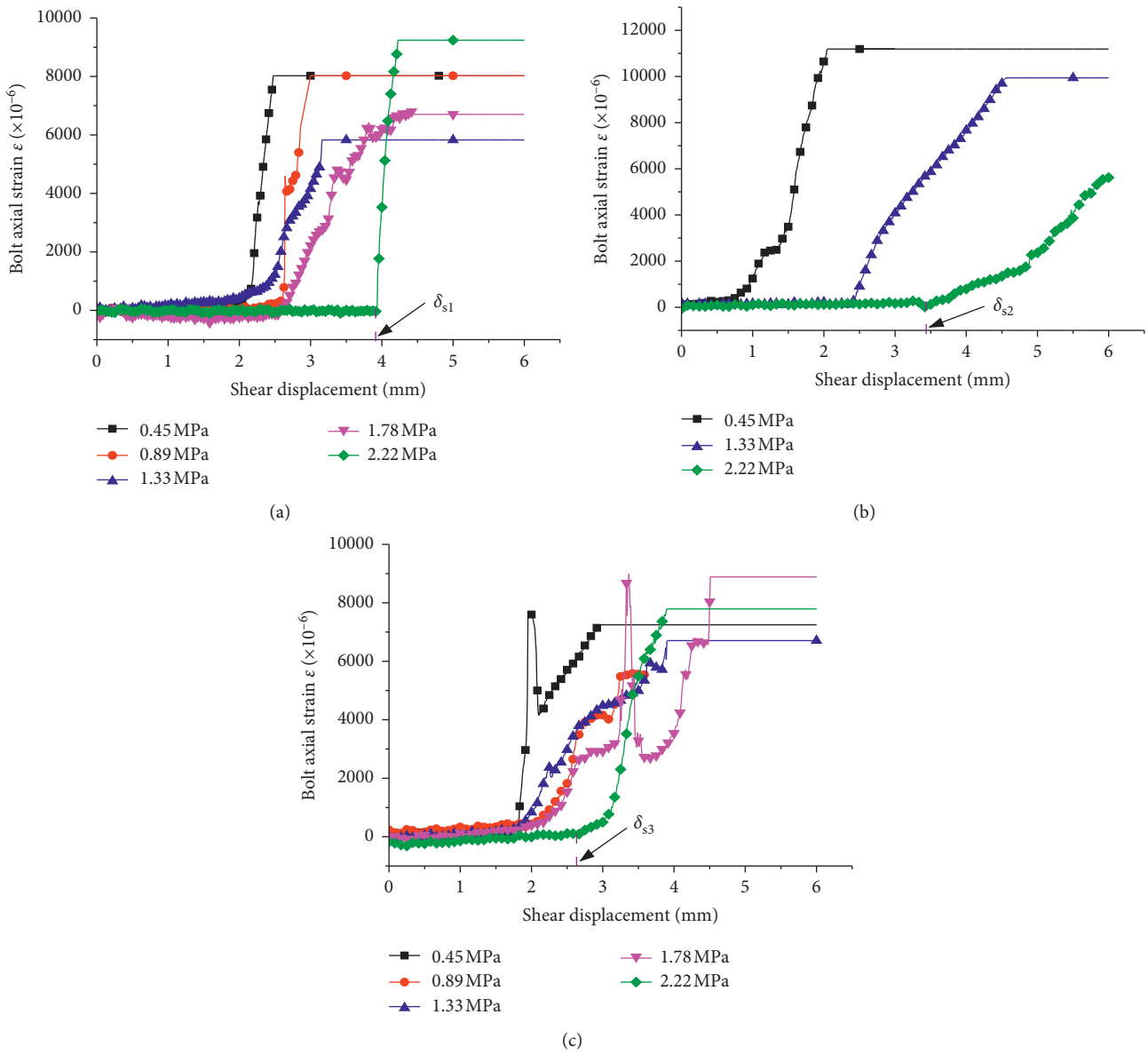

Figure 5: Strain-displacement curve of the grouted joint with one bolt (a), two bolts (b), and three bolts (c) of 45° inclination.

analysis, when the bolt strain mutates, the joint shear stress has almost reached its peak value wherein the joint is close to the destruction state. Therefore, the failure time of the grouted joint can be judged by the state of the bolt strain curve. When an abrupt change in the axial force of the bolt is detected (reaching the yield state of the bolt), the bolted system is about to destabilize.

With increased number of bolts, the yield displacement continuously decreases, $\delta_{s3} < \delta_{s2} < \delta_{s1}$. In other words, a larger number of bolts lead to a smaller yield displacement. The reason is that a smaller number of bolts result in lower bolt rigidity, causing the joint surface to be damaged first and the bolt to be damaged again. With increased number of bolts, the stiffness of the bolt system increases so that it can be destroyed simultaneously with joints, leading to early yielding displacement of the bolt. At the same number of bolts, the yield displacement of the bolt increases with increased normal load because increased normal load causes increased density of the contact of the structural surface. Subsequently, the shear stress of the joint increases gradually and the shear stress of the bolt decreases relatively. The bolt coordinates with the rock and resists shear deformation, thereby producing greater normal load and greater yield displacement of the bolt. Figure 5(c) shows that when the normal load is 0.45 and 1.78 MPa, the stress-shear displacement curve of the bolt has a sharp point. The adhesive force of the grout is large before the failure because of the shear process. With increased shear stress on the joint, the ultimate bearing capacity is reached, and the grout suddenly breaks down. At this point, the bolt is subjected to a sudden increase in shear and axial stresses. Then, when the grout is deformed, it bears part of the stress and the axial force of the bolt drops to a normal value, which is a very short process thereby forming a sharp point.

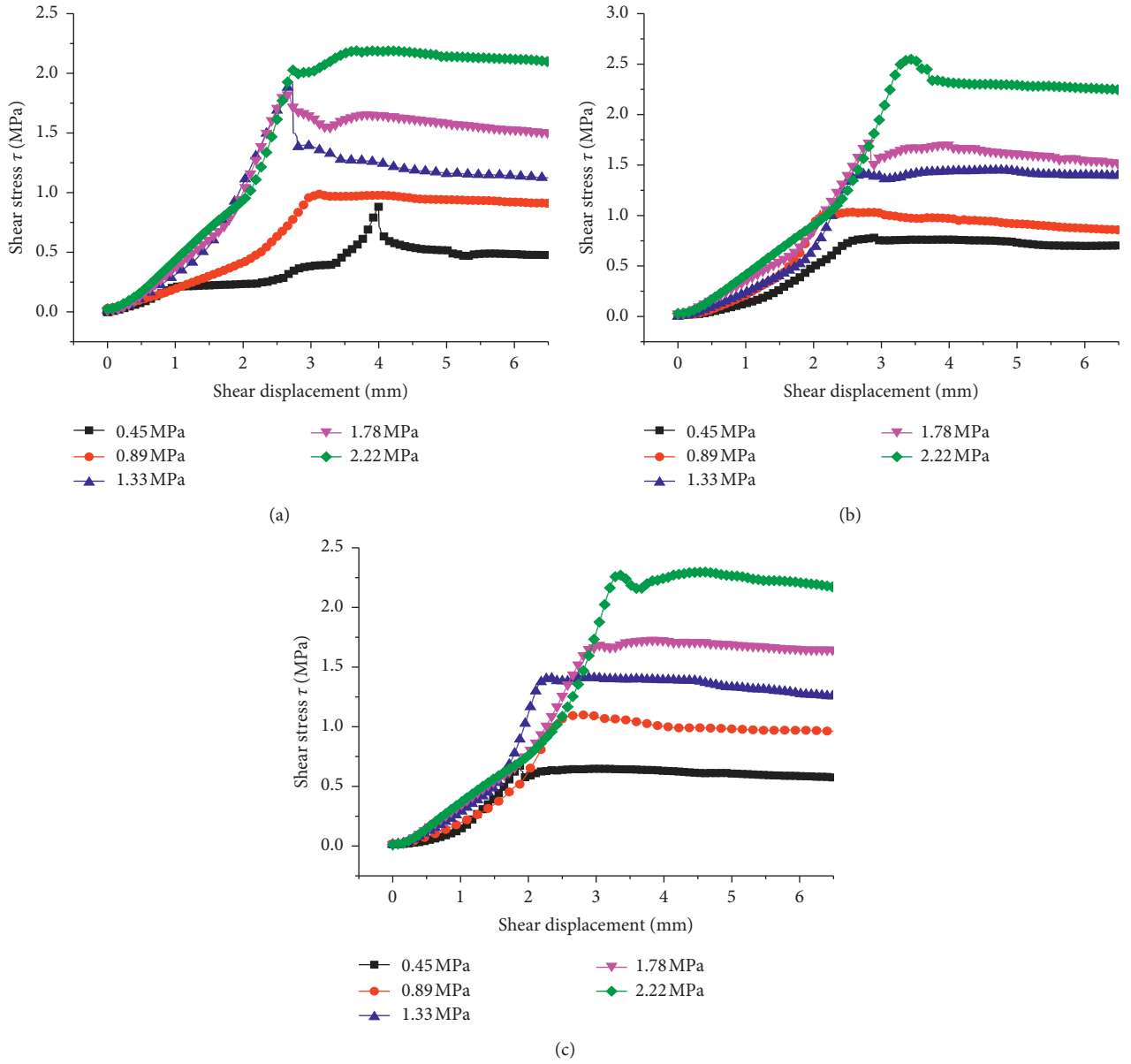

Figure 6: Shear stress-shear displacement curves of the grouted joint with one bolt (a), two bolts (b), and three bolts (c) of 45° inclination.

3.2. Effect of Grouting. The shear behavior of bolted nonfilled and bolted grouted joints was studied. The results of the direct shear tests for the joint with a 45° bolt under a different normal stress are shown in Figure 7. The yield displacement of the bolts in the grouted joint is greater than that of the nonfilled joint indicating that the grouting can increase the yield displacement of the bolt. The stiffness of the joint is relatively large, and the bolt rapidly deforms against the shear stress in the nonfilled joint. The stiffness of the bolted grouted joint is smaller than that of the bolted nonfilled joint. When the deformation of the bolt reaches the limit, the bolt begins to yield. The grout is sheared and broken during the shearing process because of the small stiffness of the grout. The grout has to have a certain thickness to provide more deformation capacity for the deformation of the bolt and to avoid the transverse shear deformation of the bolt directly. The bolt interacts with the grout and cooperates with each other to coordinate the load and increase the shear strength of the joint. According to the slope of the deformation curve of the bolt, the slope of the deformation curve of the bolt in the nonfilled joint is larger than that in the grouted joint. The slope of the curve represents the deformation speed of the bolt during shear. The higher the slope, the faster the deformation of the bolt, and the greater the axial force the bolt bears when it is deformed. After grouting, the deformation speed of the bolt decreases, and the initial time of yielding of the bolt is delayed. Reflecting grouting can improve the axial force of the bolt and improve the shear strength of the joint.

3.3. Influence of Bolt Inclination. After the joint is cut out, the deformation of the bolt is shown in Figure 8. After shearing,

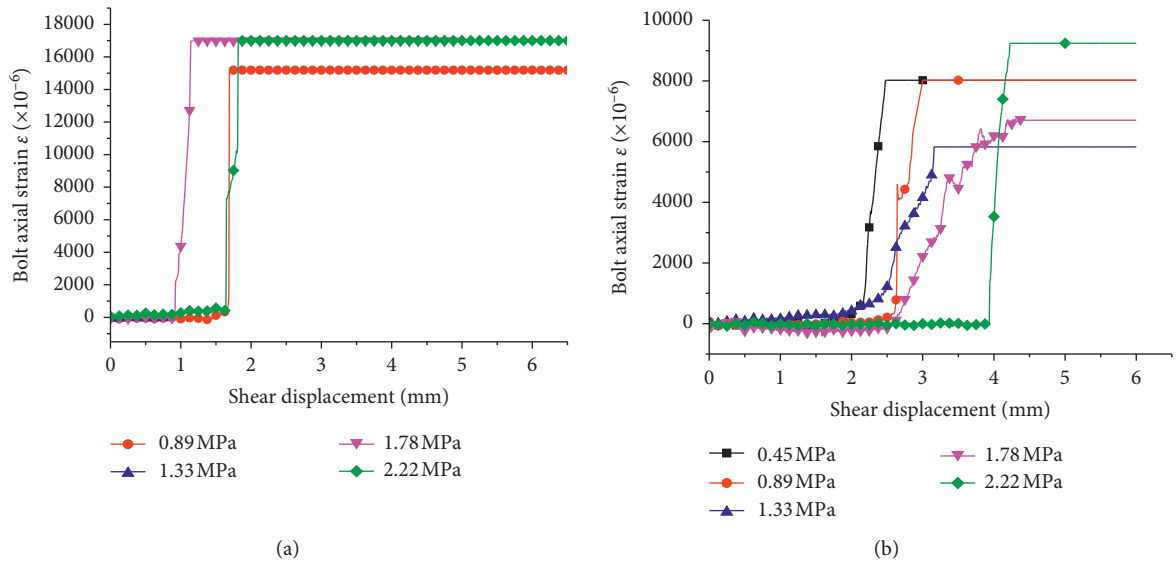

Figure 7: Strain-shear displacement curve of bolt in nonfilled joint with one bolt (a) and grouted joint with one bolt (b) of 45° inclination.

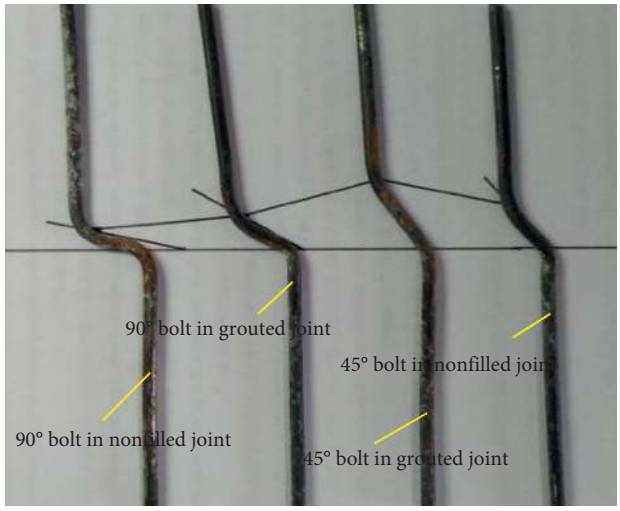

Figure 8: Deformation of the rock bolt with a different inclination.

the bending phenomenon of the bolt in the nonfilled joint is more obvious than that in the grouted joint because the grout has a certain thickness in the grouted joint. When the joint is sheared, the bolt bends at the cementing surface of the grout. In the filled grout, the bolt is stretched, whereas the bolt can only bend near the structural surface in the nonfilled joint. The 90° bolt anchorage angle is larger in the process of shearing wherein the bolt plays the role of pin and there is difficulty in removing slippage. The 45° bolt bevels the joint wherein the bolt also plays the role of axial drawing while exerting transverse shear resistance. Most of the deformation positions of the bolt are in the middle, while some are found above or below the middle.

In comparing the strain-shear displacement curves of bolts with different inclination angles (Figure 9), the axial deformation of the bolt varies with increased shear displacement. At the beginning of the bolt deformation, the 45° bolt curve slope is greater than that of the 90° bolt, while the yield displacement of the 45° bolt is smaller showing that under the condition of the same shear displacement, the 45° bolt is subjected to greater axial tension compared with the 90° bolt. The bolt axial drawing function is more apparent, and the axial pulling action of the 45° bolt is more obvious. The differences of yield displacement indicate that the 45° bolt plays a pullout role earlier than the 90° bolt because when the bolt inclination is at 90°, the bolt perpendicular to it intersects with the joint and plays the role of the transverse shear resistance, while the axial drawing is not produced until the bolt is bent and deformed. The 45° bolt bevels with the joint when the joint is staggered along the shear direction, and the bolt is subjected to the force of the rock block. To resist the force, the bolt produces axial and shear deformations. Therefore, the 45° bolt presents the better supporting effect than the 90° bolt.

3.4. Failure Mode of Joint. Under a certain normal load, the unbolted joint underwent shear deformation. When the shear stress reached the peak shear strength, the joint suffered a sliding failure [47–53]. The bolt plays an important role in the bolted joint. For the nonfilled joint, shear deformation occurs on the joint and bolt at the initial stage of shear, and the axial deformation of the bolt is not obvious. When the shear stress reaches the maximum shear strength of the joint, sliding failure occurs (Figure 10(a)). The bolt begins to yield, and the axial deformation gradually increases. The bolt produces bending and shear failure, and part of the bolt is broken at the joint as shown in Figure 11. The sliding of the joint overcomes the dynamic friction resistance and the transverse and axial resistance of the bolt. For the bolted grouted joint, both the bolt and the filled grout simultaneously undergo shear deformation at the initial state of shearing, and the axial deformation of the bolt is not obvious. When the shear stress reaches the peak shear strength of the bolted grouted joint, the filled grout is damaged and the bolt begins to yield, while the axial

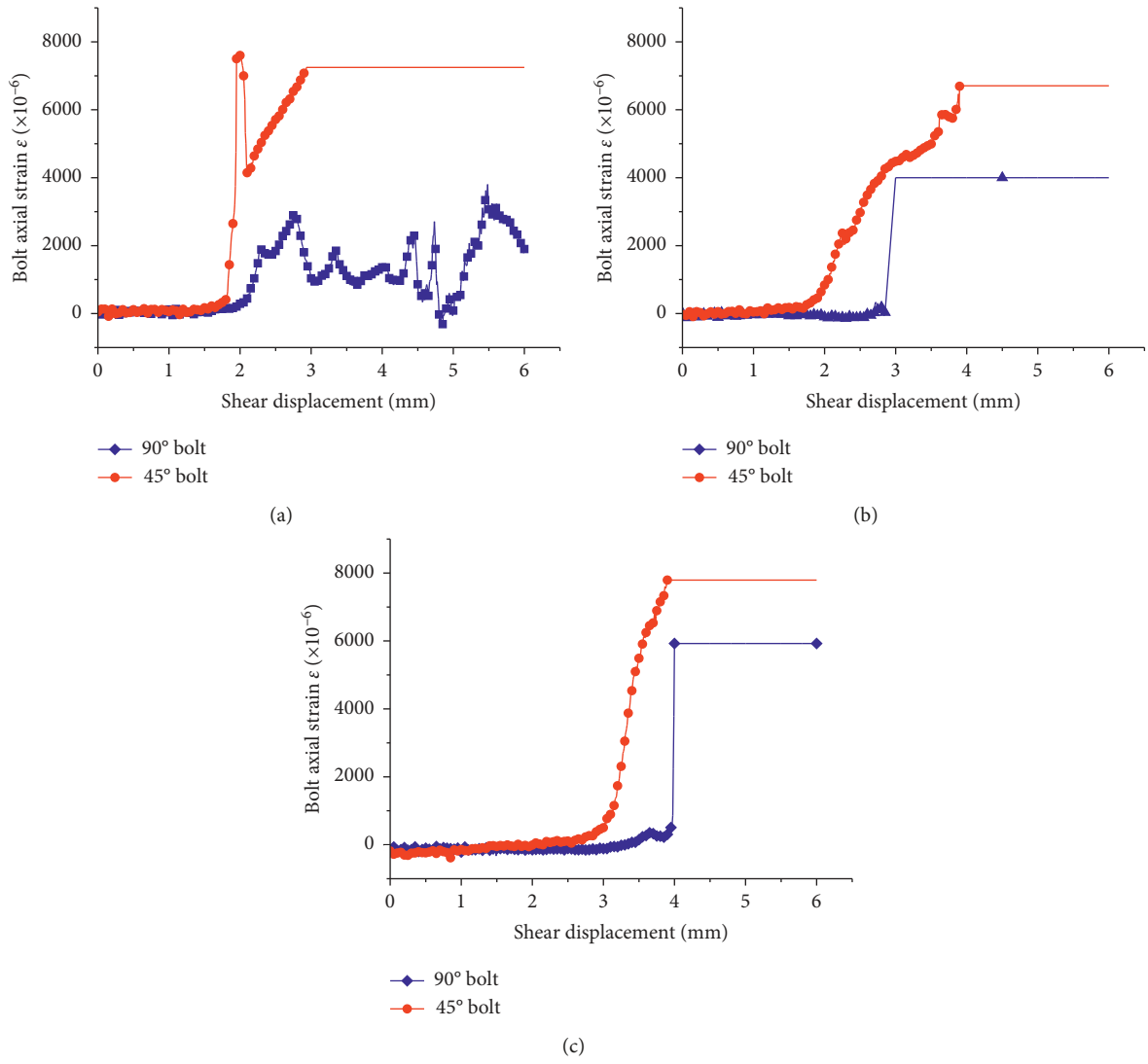

Figure 9: Strain-shear displacement curve of the bolt with a different inclination. Normal load of (a) 0.45 MPa, (b) 1.33 MPa, and (c) 2.22 MPa.

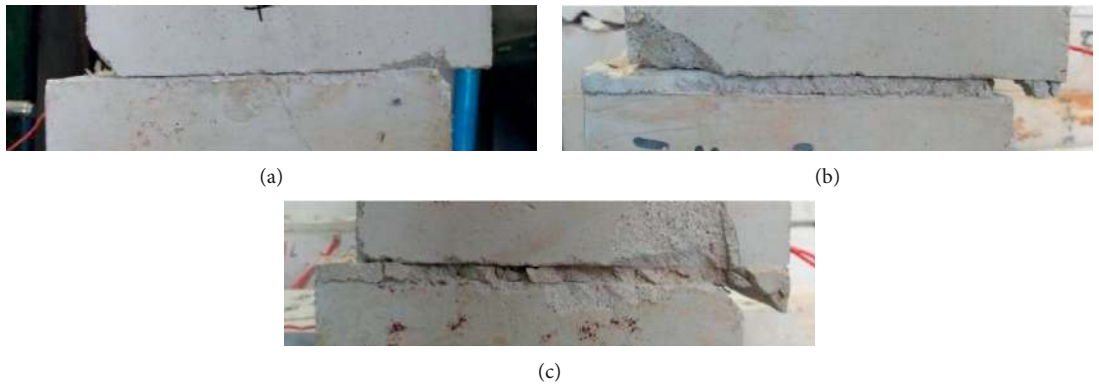

Figure 10: Failure modes of different joints. (a) Nonfilled joint. (b) Failure mode 1 of the bolted grouted joint. (c) Failure mode 2 of the bolted grouted joint.

deformation of the bolt increases gradually. There are two main types of failure modes of the joint wherein one is a sliding failure along the interface between the filled grout and the rock as shown in Figure 10(b) and another is the crushing failure of the filled grout as shown in Figure 10(c). Compared with the nonfilled joint, the bolt in the grouted

Figure 11: Broken bolt.

joint has hardly been broken, and the corresponding shear displacement of the grouted joint when the joint is damaged and the bolt begins to yield is larger than that of the nonfilled joint. The frictional resistance of the bolted grouted joint comes from the damaged filled grout. The partially broken grout occludes with each other as shown in Figure 10(c), thereby increasing the frictional resistance of the joint.

4. Conclusions

(1) With increased number of bolts, the shear strength of the joint increases and the yield displacement of the bolt decreases. The normal load increases as the yield displacement of the bolt and the shear strength of the joint increase.

(2) Grouting in the joint can improve the stress conditions of the bolt. The filled grout and the bolt work together to increase the shear strength of the joint. The stiffness of the rigid anchorage joint is large, and the anchor rod quickly yields against the shear force. The stiffness of nonfilled joint and grouted joint is relatively larger, and the bolt yields rapidly with the resistance to shear forces. The stiffness of the bolted grouted joint is relatively small, and the bolt can undergo a coordinated deformation along with the filled grout. When the deformation of the bolt reaches the limit, the bolt begins to yield.

(3) The inclination angle of the bolt has an effect on the shear strength of the joint. When the bolt inclination angle is 45°, the shear strength is greater than that of 90°. For a different inclination, the bolt plays an axial drawing role, whereas the 45° bolt plays a pullout role earlier than that of the 90° bolt.

Data Availability

The data used to support the findings of this study are available from the corresponding author upon request.

Conflicts of Interest

The authors declare that there are no conflicts of interest.

Acknowledgments

This work was supported by the National Natural Science Foundation of China (51774322); Hunan Provincial Natural Science Foundation of China (2018JJ2500); and State Key Laboratory of Mining Disaster Prevention and Control Cofounded by Shandong Province, the Ministry of Science and Technology, and Shandong University of Science and Technology (MDPC201814). The authors wish to acknowledge these supports.

References

[1] J. Shen and R. Jimenez, "Predicting the shear strength parameters of sandstone using genetic programming," *Bulletin of Engineering Geology and the Environment*, vol. 77, no. 4, pp. 1647–1662, 2018.

[2] R. Yong, J. Ye, S.-G. Du, H. Zhang, L. Gu, and H. Lin, "A dice similarity measure for TBM penetrability classification in hard rock condition with the intuitionistic fuzzy information of rock mass properties," *European Journal of Environmental and Civil Engineering*, vol. 24, pp. 1–16, 2020.

[3] H. Lin, H. Wang, X. Fan, P. Cao, and K. Zhou, "Particle size distribution effects on deformation properties of graded aggregate base under cyclic loading," *European Journal of Environmental and Civil Engineering*, vol. 23, no. 3, pp. 269–286, 2019.

[4] Y. Wang, H. Lin, Y. Zhao, X. Li, P. Guo, and Y. Liu, "Analysis of fracturing characteristics of unconfined rock plate under edge-on impact loading," *European Journal of Environmental and Civil Engineering*, vol. 24, pp. 1–16, 2020.

[5] Y. Chen and H. Lin, "Consistency analysis of Hoek-Brown and equivalent Mohr-coulomb parameters in calculating slope safety factor," *Bulletin of Engineering Geology and the Environment*, vol. 78, no. 6, pp. 4349–4361, 2019.

[6] Z. Wen, S. Jing, Y. Jiang et al., "Study of the fracture law of overlying strata under water based on the flow-stress-damage model," *Geofluids*, vol. 2019, Article ID 3161852, 12 pages, 2019.

[7] Y. Zhao, L. Zhang, W. Wang, J. Tang, H. Lin, and W. Wan, "Transient pulse test and morphological analysis of single rock fractures," *International Journal of Rock Mechanics & Mining Sciences*, vol. 91, pp. 139–154, 2017.

[8] Q. Lin, P. Cao, and R. Cao, "Experimental investigation of jointed rock breaking under a disc cutter with different confining stresses," *Comptes Rendus Mécanique*, vol. 346, no. 9, pp. 833–843, 2018.

[9] M. Jiang, J. Liu, G. B. Crosta, and T. Li, "DEM analysis of the effect of joint geometry on the shear behavior of rocks," *Comptes Rendus Mécanique*, vol. 345, no. 11, pp. 779–796, 2017.

[10] C. Zhang, C. Pu, R. Cao, T. Jiang, and G. Huang, "The stability and roof-support optimization of roadways passing through unfavorable geological bodies using advanced detection and monitoring methods, among others, in the Sanmenxia Bauxite Mine in China's Henan Province," *Bulletin of Engineering Geology and the Environment*, vol. 78, no. 7, pp. 5087–5099, 2019.

[11] D. Lei, H. Lin, Y. Chen, R. Cao, and Z. Wen, "Effect of cyclic freezing-thawing on the shear mechanical characteristics of nonpersistent joints," *Advances in Materials Science and Engineering*, vol. 2019, no. 6, 14 pages, 2018.

[12] H. Lin, W. Xiong, Z. Xiong, and F. Gong, "Three-dimensional effects in a flattened Brazilian disk test," *International Journal of Rock Mechanics and Mining Sciences*, vol. 74, pp. 10–14, 2015.

[13] M. O'Neill, D. Cafiso, R. Mala, G. La Rosa, and D. Taylor, "Fracture toughness and damage development in limpet shells," *Theoretical and Applied Fracture Mechanics*, vol. 96, pp. 168–173, 2018.

[14] S. Pirmohammad and M. Hojjati Mengharpey, "A new mixed mode I/II fracture test specimen: numerical and experimental studies," *Theoretical and Applied Fracture Mechanics*, vol. 97, pp. 204–214, 2018.

[15] J. S. Sim, T. S. Kang, Y. T. Lee, and H. J. Kim, "Analysis for mechanical behavior of GFRP rock bolt for permanent support of tunnel," *Pharmacology & Therapeutics*, vol. 14, no. 6, pp. 91–105, 2010.

[16] W. Wang, Q. Song, C. Xu, and H. Gong, "Mechanical behaviour of fully grouted GFRP rock bolts under the joint action of pre-tension load and blast dynamic load," *Tunnelling and Underground Space Technology*, vol. 73, pp. 82–91, 2018.

[17] G. Mostafa, S. Kourosh, and J. Hossein, "Analysis profile of the fully grouted rock bolt in jointed rock using analytical and numerical methods," *International Journal of Mining Science and Technology*, vol. 24, no. 5, pp. 609–615, 2014.

[18] Y.-X. Wang, P.-P. Guo, W.-X. Ren et al., "Laboratory investigation on strength characteristics of expansive soil treated with jute fiber reinforcement," *International Journal of Geomechanics*, vol. 17, no. 11, Article ID 04017101, 2017.

[19] H.-Y. Fu, Z.-M. Jiang, and H.-Y. Li, "Physical modeling of compressive behaviors of anchored rock masses," *International Journal of Geomechanics*, vol. 11, no. 3, pp. 186–194, 2011.

[20] A. Showkati, P. Maarefvand, and H. Hassani, "An analytical solution for stresses induced by a post-tensioned anchor in rocks containing two perpendicular joint sets," *Acta Geotechnica*, vol. 11, no. 2, pp. 415–432, 2016.

[21] S. Ma, J. Nemcik, and N. Aziz, "Simulation of fully grouted rockbolts in underground roadways using FLAC2D," *Canadian Geotechnical Journal*, vol. 51, no. 8, pp. 911–920, 2014.

[22] S. Sakurai, "Modeling strategy for jointed rock masses reinforced by rock bolts in tunneling practice," *Acta Geotechnica*, vol. 5, no. 2, pp. 121–126, 2010.

[23] Y. Wang, P. Guo, H. Lin et al., "Numerical analysis of fiber-reinforced soils based on the equivalent additional stress concept," *International Journal of Geomechanics*, vol. 19, no. 11, 2019.

[24] Y. Wang, P. Guo, X. Li, H. Lin, Y. Liu, and H. Yuan, "Behavior of fiber-reinforced and lime-stabilized clayey soil in triaxial tests," *Applied Sciences*, vol. 9, no. 5, p. 900, 2019.

[25] X. Chen, N. Zhang, T. Ma, X. Niu, X. Liu, and T. Feng, "Energy-based forming and anchoring mechanism and criterion for zonal disintegration," *Theoretical and Applied Fracture Mechanics*, vol. 97, pp. 349–356, 2018.

[26] X. Wu, Y. Jiang, B. Gong, Z. Guan, and T. Deng, "Shear performance of rock joint reinforced by fully encapsulated rock bolt under cyclic loading condition," *Rock Mechanics and Rock Engineering*, vol. 52, no. 8, pp. 2681–2690, 2019.

[27] Z. Wen, E. Xing, S. Shi, and Y. Jiang, "Overlying strata structural modeling and support applicability analysis for large mining-height stopes," *Journal of Loss Prevention in the Process Industries*, vol. 57, pp. 94–100, 2019.

[28] X. Ge and J. Liu, "Study on the shear resistance behaviour of bolted rock joints," *Chinese Jounal of Geotechnical Engineering*, vol. 10, no. 1, pp. 8–19, 1988.

[29] W. Q. Chen, Z. X. Jia, Y. F. Zhao, L. P. Liu, J. J. Zhou, and X. C. Lin, "Analysis of axial and transverse effects of rock bolt during shearing process," *Rock & Soil Mechanics*, vol. 36, no. 1, pp. 143–148, 2015.

[30] K. Spang and P. Egger, "Action of fully-grouted bolts in jointed rock and factors of influence," *Rock Mechanics and Rock Engineering*, vol. 23, no. 3, pp. 201–229, 1990.

[31] F. Pellet and P. Egger, "Analytical model for the mechanical behaviour of bolted rock joints subjected to shearing," *Rock Mechanics and Rock Engineering*, vol. 29, no. 2, pp. 73–97, 1996.

[32] C. J. Haas, "Shear resistance of rock bolts," *Transactions of the Society of Mining Engineers of AIME*, vol. 260, no. 1, pp. 32–41, 1976.

[33] G. Grasselli, M. Kharchafi, and P. Egger, "Experimental and numerical comparison between fully grouted and frictional bolts," in *Proceedings of the International Society for Rock Mechanics and Rock Engineering*, Paris, France, August 1999.

[34] M. Ranjbarnia, A. Fahimifar, and P. Oreste, "Practical method for the design of pretensioned fully grouted rockbolts in tunnels," *International Journal of Geomechanics*, vol. 16, no. 1, Article ID 04015012, 2016.

[35] D. Deb and K. C. Das, "A new doubly enriched finite element for modelling grouted bolt crossed by rock joint," *International Journal of Rock Mechanics and Mining Sciences*, vol. 70, no. 9, pp. 47–58, 2014.

[36] S. Maghous, D. Bernaud, and E. Couto, "Three-dimensional numerical simulation of rock deformation in bolt-supported tunnels: a homogenization approach," *Tunnelling and Underground Space Technology*, vol. 31, pp. 68–79, 2012.

[37] H. Lin, X. Ding, R. Yong, W. Xu, and S. Du, "Effect of non-persistent joints distribution on shear behavior," *Comptes Rendus Mécanique*, vol. 347, no. 6, pp. 477–489, 2019.

[38] X. Fan, H. Lin, H. Lai, R. Cao, and J. Liu, "Numerical analysis of the compressive and shear failure behavior of rock containing multi-intermittent joints," *Comptes Rendus Mécanique*, vol. 347, no. 1, pp. 33–48, 2019.

[39] R. Sahlaoui, K. Sab, and J.-V. Heck, "Yield strength of masonry-like structures containing thin adhesive joints: 3D or 2D-interface model for the joints?," *Comptes Rendus Mécanique*, vol. 339, no. 6, pp. 432–438, 2011.

[40] Y. Shen, Y. Wang, Y. Yang, Q. Sun, T. Luo, and H. Zhang, "Influence of surface roughness and hydrophilicity on bonding strength of concrete-rock interface," *Construction and Building Materials*, vol. 213, pp. 156–166, 2019.

[41] Y.-J. Shen, G.-S. Yang, H.-W. Huang, T.-L. Rong, and H.-L. Jia, "The impact of environmental temperature change on the interior temperature of quasi-sandstone in cold region: experiment and numerical simulation," *Engineering Geology*, vol. 239, pp. 241–253, 2018.

[42] C. Jiang, Y. Li, L. Liu, H. Lin, and J. He, "The undrained vertical and horizontal bearing capacity of internal skirted foundation in clay," *European Journal of Environmental and Civil Engineering*, vol. 36, no. 6, pp. 1–13, 2018.

[43] H. Lin, H. Yang, Y. Wang, Y. Zhao, and R. Cao, "Determination of the stress field and crack initiation angle of an open flaw tip under uniaxial compression," *Theoretical and Applied Fracture Mechanics*, vol. 104, p. 102358, 2019.

[44] X. Wu, Y. Jiang, B. Gong, T. Deng, and Z. Guan, "Behaviour of rock joint reinforced by energy-absorbing rock bolt under cyclic shear loading condition," *International Journal of Rock Mechanics and Mining Sciences*, vol. 110, pp. 88–96, 2018.

[45] H. Lin, Z. Xiong, T. Liu, R. Cao, and P. Cao, "Numerical simulations of the effect of bolt inclination on the shear strength of rock joints," *International Journal of Rock Mechanics and Mining Sciences*, vol. 66, no. 1, pp. 49–56, 2014.

[46] Y. Chen, P. Cao, K.-p. Zhou, and Y. Teng, "Relationship between loading angle and displacing angle in steel bolt shearing," *Transactions of Nonferrous Metals Society of China*, vol. 27, no. 4, pp. 876–882, 2017.

[47] R.-h. Cao, P. Cao, H. Lin, G. Ma, and Y. Chen, "Failure characteristics of intermittent fissures under a compressive-

shear test: experimental and numerical analyses," *Theoretical and Applied Fracture Mechanics*, vol. 96, pp. 740–757, 2018.

[48] H. Wang and H. Lin, "Non-linear shear strength criterion for a rock joint with consideration of friction variation," *Geotechnical and Geological Engineering*, vol. 36, no. 6, pp. 3731–3741, 2018.

[49] T.-H. Kwon, E.-S. Hong, and G.-C. Cho, "Shear behavior of rectangular-shaped asperities in rock joints," *KSCE Journal of Civil Engineering*, vol. 14, no. 3, pp. 323–332, 2010.

[50] H. S. Lee, Y. J. Park, T. F. Cho, and K. H. You, "Influence of asperity degradation on the mechanical behavior of rough rock joints under cyclic shear loading," *International Journal of Rock Mechanics and Mining Sciences*, vol. 38, no. 7, pp. 967–980, 2001.

[51] H. Lin, S. Xie, R. Yong, Y. Chen, and S. Du, "An empirical statistical constitutive relationship for rock joint shearing considering scale effect," *Comptes Rendus Mécanique*, vol. 347, no. 8, pp. 561–575, 2019.

[52] M. Heshmati, R. Haghani, M. Al-Emrani, and A. André, "On the strength prediction of adhesively bonded FRP-steel joints using cohesive zone modelling," *Theoretical and Applied Fracture Mechanics*, vol. 93, pp. 64–78, 2018.

[53] P. Štefane, S. Naib, S. Hertelé, W. De Waele, and N. Gubeljak, "Crack tip constraint analysis in welded joints with pronounced strength and toughness heterogeneity," *Theoretical and Applied Fracture Mechanics*, vol. 103, Article ID 102293, 2019.